Analysis of large-area twins in $Bi_2CaSr_2Cu_2O_8$ superconductors

P. D. Han, A. Asthana, Z. Xu, L. Chang, and D. A. Payne
Department of Materials Science and Engineering, Materials Research Laboratory, University of Illinois at Urbana-Champaign, Urbana, Illinois 61801
(Received 6 July 1990; revised manuscript received 5 November 1990)

We report on large-area twin structures in $Bi_2CaSr_2Cu_2O_8$. Crystal growth was by a self-fluxed method. Twins were extracted from the free surfaces of the resolidified flux. Twinning was characterized by optical microscopy, scanning electron microscopy, and transmission electron microscopy and the twins were determined to be growth twins with {110} twin boundaries. Details of twin morphology and structure are presented in the context of twin formation and growth. Superconducting properties of the twinned specimens were determined by electrical and magnetic measurements. Preliminary results indicate that a single twin boundary did not significantly affect the resistance-temperature characteristics. Growth steps on the (001) face (which necessitated current transport in the **c** direction) were more important in determining the sharpness and form of the resistive transition.

INTRODUCTION

Several families of oxide superconductors (e.g., Y-Ba-Cu-O, Bi-Ca-Sr-Cu-O, and Tl-Ba-Sr-Cu-O) have been discovered in recent years with T_c's above the boiling point of liquid nitrogen.[1-3] A common feature is that they are comprised of unit cells with one or more CuO_2 layers sandwiched between perovskitelike metal-oxygen layers. The crystals have a characteristic layer-growth morphology with strong anisotropy in properties. An understanding of the features of crystallization and growth, and their interrelationships with superconducting properties, is desirable. From this point of view, an interesting question is the role of crystallographic defects (such as, twins, syntactic intergrowths, etc.) on properties. In this paper we report on the effects of twin walls and growth steps on superconducting properties.

There are three known superconducting phases in the Bi-Ca-Sr-Cu-O homologous series $(BiO)_2Ca_{n-1}Sr_2Cu_nO_{2n+2}$ $(n=1,2,3)$.[4-7] The 2:1:2:2 phase ($Bi_2CaSr_2Cu_2O_8$, $n=2$) has a $T_c \sim 80$ K and a pseudotetragonal subcell, with $\mathbf{a} \approx \mathbf{b} = 5.40$ Å and $\mathbf{c} = 30.89$ Å. There is an incommensurate superstructure arising from modulated displacements of Bi atoms. The modulated structure may be described in terms of an orthorhombic superlattice.[5,6,8-15] We have chosen the **b** axis as the direction of the incommensurate modulation, in agreement with several authors.[5,8-12] (However, some authors describe the structure on the basis of *Amaa* or *A*2*aa* space-group assignments, with the **a** axis as the direction of modulation.[6,13-15]) Regardless of the exact space group assignment, (110) twins are to be expected from symmetry considerations for an orthorhombic structure. Evidence of twins may give important clues to the mechanism of crystal growth and superconductivity. For example, coherent twin boundaries could be associated with (i) pinning sites for magnetic flux, (ii) hole-absent sites necessary for the delocalization of hole pairs, and (iii) nucleation sites for the transition from normal to superconducting states.[16]

Recently we reported[17] the existence of large-scale (110) twins in $Bi_2CaSr_2Cu_2O_8$. In the present investigation we report on the shape and form of the twins which were grown under near-equilibrium conditions (i.e., in contact with a free surface and at very low growth rates). An analysis of twinning is presented, as determined by optical and electron microscopy. The twins were determined to be growth twins. Preliminary results on the possible effects of twinning on superconducting properties are given.

EXPERIMENTAL METHOD

Crystals of 2:1:2:2 phase were grown by a self-fluxed method in a temperature gradient.[18] Powders of Bi_2O_3, $CaCO_3$, $SrCO_3$, and CuO were weighed in the ratio [Bi]:[Ca]:[Sr]:[Cu]=2:1.5:1.5:2.6, and mixed thoroughly in a mortar and pestle. The starting materials were greater than 99.99% pure. The mixture was fused in a MgO crucible (100 cm^3) at 990 °C and equilibrated for 6 hr in air. The temperature was then rapidly decreased to 875–880 °C, in order to provide sufficient supercooling for nucleation. After a further equilibration for 6 hr, the temperature was slowly cooled at 0.5–2 °C/hr to 790 °C where crystal growth was terminated. A small temperature gradient (~5 °C/cm) and fine porosity in the crucible helped to create cavities within the resolidified flux. Several flux-free crystals and twins, 1–4 mm in size, could be extracted from the free surface or from within the cavities.

A Leitz hot-stage microscope, equipped with a 100-watt halogen lamp and a microphotometer, was used for optical examination in reflected polarized light. Details of crystal morphology were examined on a Hitachi-S800 scanning electron microscope (SEM), equipped with a LINK energy-dispersive spectrometer (EDS) system. A

Philips-400T transmission electron microscope (TEM) was used for the determination of crystallographic directions (i.e., **a** and **b** axes) in the basal (001) plane of the twins by selected-area diffraction (SAD). Miller indices were assigned on the basis of a pseudotetragonal subcell of approximately 5.4 Å×5.4 Å×30.8 Å. A Quantum Design superconducting quantum interference device (SQUID) magnetometer (operated under zero-field cooling conditions at 10 Oe) and a four-point probe method (using a lockin-detection scheme with an excitation current of 0.5 mA and a voltage resolution of 5 nV at a frequency of 532 Hz) were used to characterize the magnetic and resistive transitions.

RESULTS

Crystals of 2:1:2:2 exhibit bireflectance off the basal (001) plane, in accordance with biaxial optical anisotropy between the **X** and **Y** principal vibration directions, which were later confirmed to be collinear with the **a** and **b** crystallographic axes by electron microscopy. The twins were examined under crossed polarizers in an optical microscope such that the direction of the **E** vector of the incident polarized light was parallel to the [110] direction of the sample. Figure 1 gives optical photographs of a twinned specimen of 2:1:2:2 which had a $T_c \sim 80$ K. Figure 1(a) is for normal white light reflected off the (001) surface. A near-square form with characteristic layer-growth morphology and regular growth steps is shown. Figure 1(b) is an optical photograph in cross polarized light indicating extinction in the diagonal segments of the same specimen. Complete extinction was observed on rotation of the analyzer 2.5–3° counterclockwise from the crossed-polars position. Figure 1(c) illustrates extinction for the other diagonal segments, on clockwise rotation of the analyzer from the cross-polars position. A rotation angle (η) of 2.5–3° for complete extinction was observed again. The above observations indicated 90° cruciform twinning with (110) type twin boundaries. However, it was not possible to uniquely determine the **a** and **b** crystallographic axes for each twin by optical microscopy.

The **a** and **b** axes could be distinguished by selected-area electron diffraction (SAD) in the TEM due to the weaker satellite spots arising from an about fivefold superlattice along the [010] direction. SAD patterns for the twin boundary, and the single-twin regions on either side of the twin boundary, are given in Fig. 2. SAD patterns from individual twins were similar but rotated 90° with respect to one another. The diffraction pattern for the twin boundary can be considered in terms of an overlap of the two previous patterns, as expected. SAD analysis confirmed (i) 90° (i.e., **a**-**b**) twins with a common [110] twin boundary and (ii) the **a** axis was parallel to the edges of the specimen, while the **b** axis was perpendicular to the edges.

A polarized light microscope equipped with a microphotometer was used to determine the optical anisotropy reflectance ratio. First, polarized white light with the **E** vector parallel to the **a** axis was focused with a single twin and the reflectance r_a for the **a** direction measured. The sample was then rotated such that the **E** vector of the polarized light was parallel to the **b** axis, and the procedure repeated. The optical-anisotropy ratio is given by $(r_b/r_a)^{1/2}$, where r_a and r_b refer to the reflectances along the **a** and **b** axes, respectively. The average optical-anisotropy ratio determined in this manner from 10 measurements in white light was 1.10 ± 0.05.

Figure 3 is a SEM photomicrograph of the boundary

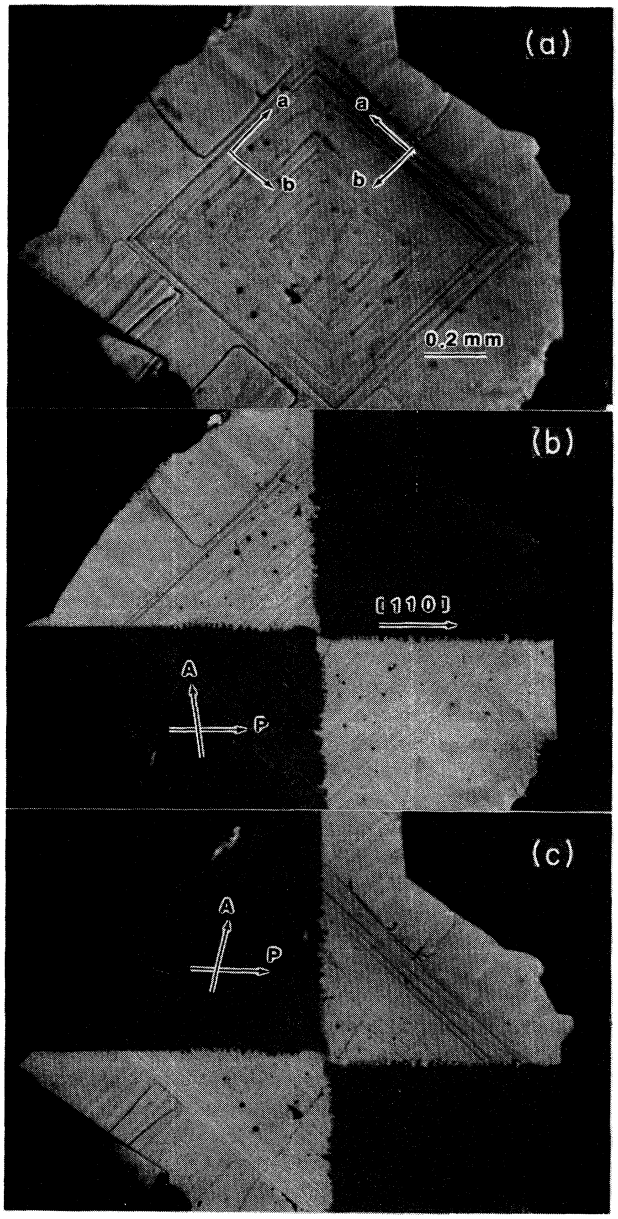

FIG. 1. Optical photomicrographs in reflected light of a cruciform twinned specimen of 2:1:2:2. (a) A characteristic near-square shape with layer growth steps parallel to [100] on the (001) face are visible in normal light. (b) Extinction of one-half (quadrants 1 and 3) was obtained between crossed polars. (Complete extinction occurred on rotation of the analyzer by 2.5–3° counterclockwise to the crossed-polars position.) (c) Extinction of the other half (quadrants 2 and 4) was obtained on rotation of the analyzer by 2.5–3° clockwise from the crossed-polars position (polarizer parallel to the [110] direction).

region. A characteristic layered structure, suggestive of two-dimensional growth, is observed. Closer examination indicates the following features: (i) several thin layers combined to form a thicker layer. The individual thin layers were 100–500 Å thick and the thicker layers were typically 0.2–0.5 μm and (ii) the layers were not in perfect registry, which was brought about by a shift in the [110] direction between each layer. Therefore, the twin boundary (given by the [110] direction) is also slightly shifted for each layer, resulting in a wider and more diffuse appearance when observed under the optical microscope (Fig. 1). An interesting feature in the above structure lies in the small region where the layers are not in perfect registry. In this local area, the (001) plane is in contact with two 90°-rotated layers (**a** and **b** axes reversed with respect to one another) and hence, serves as a 90° twist boundary or a local (001) composition plane.

When the specimen was heated in a hot-stage optical microscope (OM) from room temperature to the melting point (~880 °C), no change in twin structure was observed. This indicated the twins were growth twins, and not transformation twins. However, in a narrow temperature range between 450 and 500 °C, a decrease in contrast ratio was noted. The reason for this is not known.

Electrical resistance measurements were carried out on a twinned specimen by a four-point-probe method. The sample had a square shape with [100] growth steps, 1–5 μm in height. The effect of a single twin boundary on the electrical resistivity was determined on a triangular sample (3 mm×3 mm×0.05 mm) containing only one (110) twin boundary [see Fig. 4(a)]. The sample was fixed to a glass slide with wax and cut into a triangular form with a sharp knife under a microscope. Care was taken during sample preparation to avoid any cleavage or deformation. Electrodes were applied to the sample by silver paste and gold wire (diameter=50 μm). The contact area was less than 0.04 mm^2 and the contact resistance between the sample and the electrode was less than 0.5 Ω after a half-hour anneal in air at 650 °C. The temperature dependence of normalized resistance ($R/R_{150\,K}$) is given in Fig. 4(b) for several voltage-current configurations. The configurations correspond to different current paths in the crystal, as shown in Fig. 4(a). It may be noted that there are no significant differences in T_c when the potential drop is measured across the twin boundary or within the same twin, as long as the voltage measurement is not across different steps. For example, the voltage was measured between points on the same growth step within the

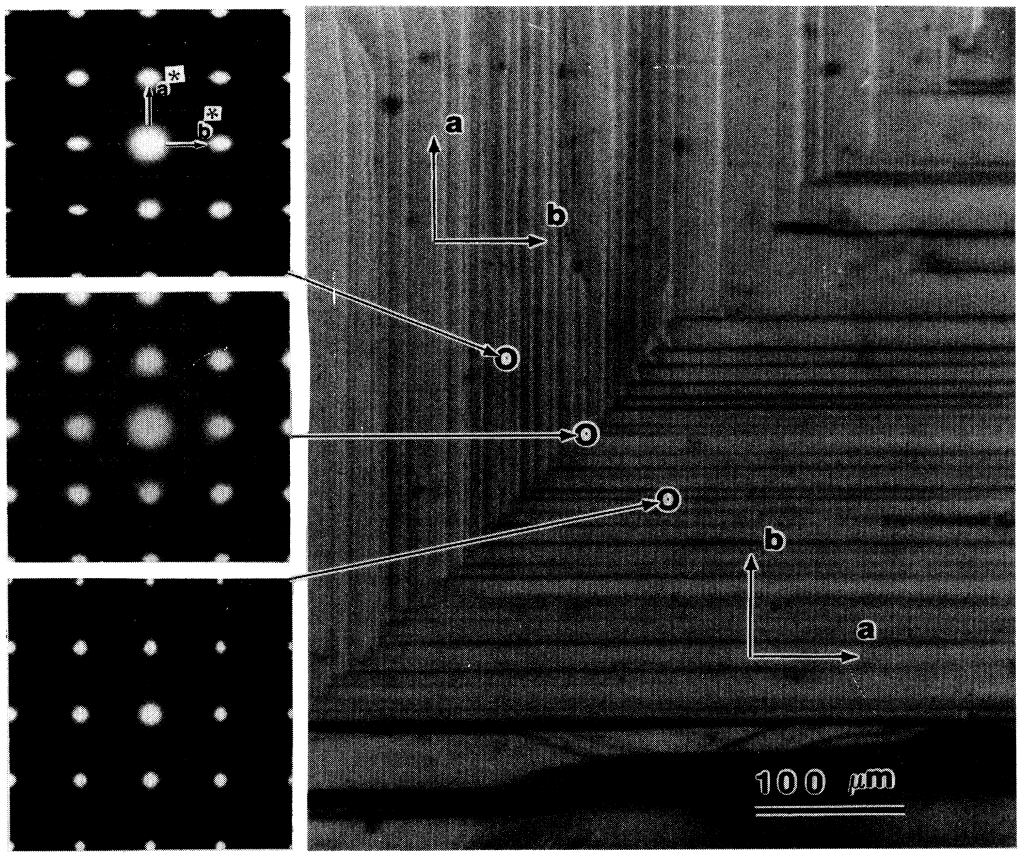

FIG. 2. (001) SAD patterns obtained from different positions in a twinned specimen. The **a** and **b** axes may easily be distinguished by the satellite spots arising from an about fivefold modulation along the [010] direction. Note that the patterns on either side of the twin boundary are similar but rotated 90° with respect to one another. The SAD pattern for the twin boundary is an overlap of the previous two patterns, as expected.

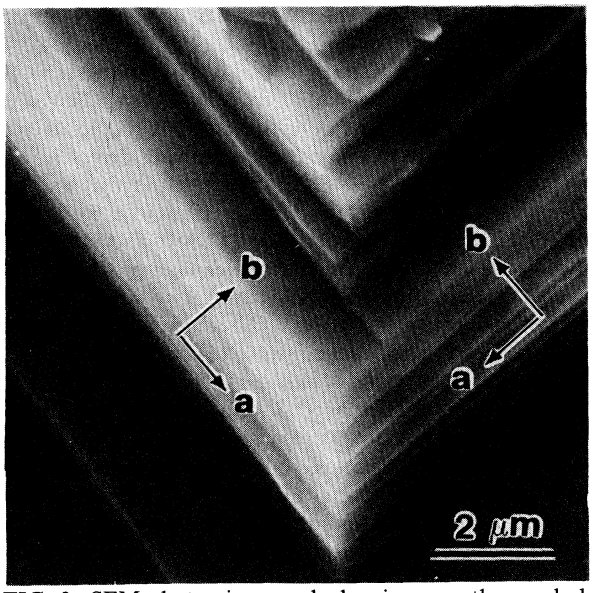

FIG. 3. SEM photomicrograph showing growth morphology of a twinned specimen. A characteristic layered structure, indicative of two-dimensional growth, is apparent. Note the disregistry between the individual growth steps, and consequent shift in the [110] boundaries, between the layers. The [110] twin boundary follows a zigzag path, as previously observed in Fig. 1.

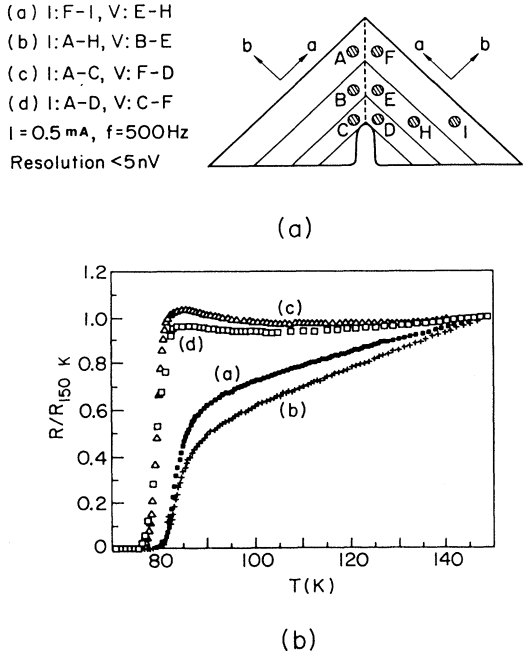

FIG. 4. (a) Schematic diagram of a twinned specimen with a single twin boundary and several growth steps. Eight electrodes (contact area <0.04 mm^2) were attached to the specimen for resistance measurements. Note, the four current-voltage configurations correspond to different current paths through the sample. (b) Resistance vs temperature characteristics for the four configurations above. The passage of current through different growth steps gives rise to the increase in resistance before the onset to zero resistance.

same twin (a) and across the twin boundary (b). The voltage probes in both cases were on the same growth step, and hence the resistance behavior was similar as a function of temperature. In (c) and (d), the potential was measured across the twin boundary and within the same twin, respectively. For this case, current transport was in the **c** direction and a rise in the resistivity-temperature characteristics was noted before the onset to zero resistance.

So as to verify the above observations, electrical measurements were carried out on a single crystal (i.e., free of twins) from the same batch. Figure 5 gives the temperature dependence of resistance for 2:1:2:2 ($2\times3\times0.05$ mm^3) along the **a**, **b**, and **c** directions. Significantly higher room-temperature resistivity along the **c** axis was noted, compared with the in-plane resistivity ($\rho_c/\rho_{ab} > 1000$), and semiconductorlike behavior before the onset of the transition. Similar anisotropy in resistance characteristics has been reported by other investigators.[19]

To summarize, preliminary measurements indicate that a single twin boundary did not significantly affect the resistance-temperature characteristics across the 2:1:2:2 twins. Rather, the transport of current in the **c** direction was more important in determining the sharpness and curvature of the resistive transition.

Figure 6 gives zero-field-cooled magnetic susceptibility versus temperature data. It is difficult to compare magnetization data between twins and single crystal specimens due to uncertainties in the demagnetization factor, shape effects, intergrowth content, etc. However, a qualitative comparison indicated no significant differences in the T_c (onset) and general behavior of the temperature dependence of magnetic susceptibilities for twins and crystals. This may be explained by noting that a single twin boundary has a small area in comparison with the

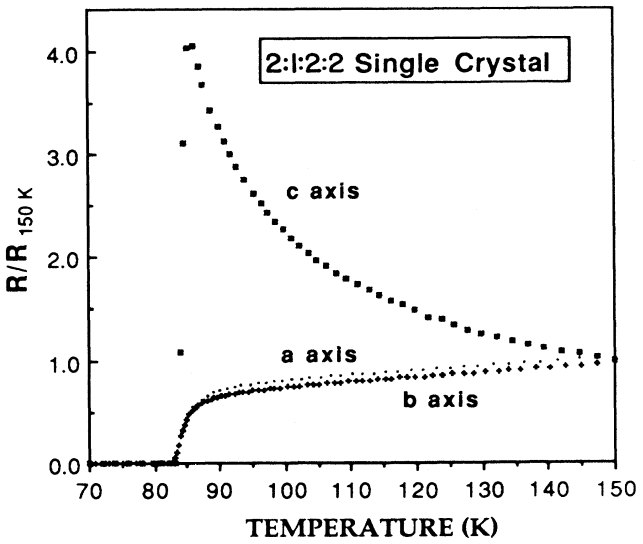

FIG. 5. Resistance vs temperature characteristics along **a**, **b**, and **c** directions for a 2:1:2:2 single crystal (i.e., twin-free).

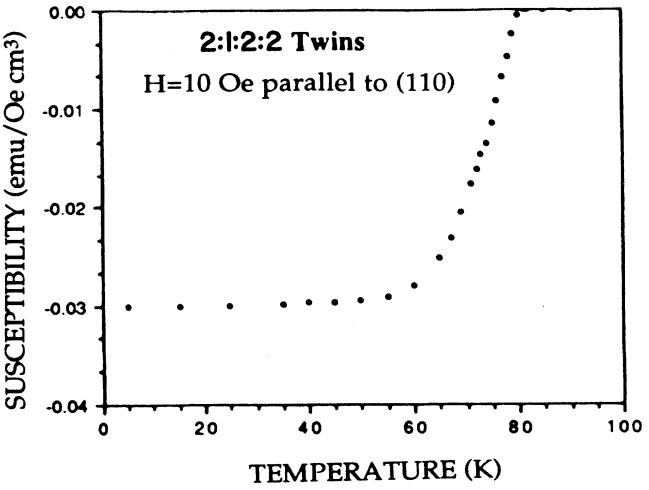

FIG. 6. Magnetic susceptibility vs temperature characteristics for a twinned specimen.

crystal volume and hence, cannot significantly affect the diamagnetic properties.

DISCUSSION

Contrast formation for twinned specimens examined in cross-polarized light may be understood from Fig. 7,[20] where **A** and **P** denote the analyzer and polarizer directions, respectively. When linear polarized light impinges with its **E** vector parallel to **P** onto an absorbing and bireflecting surface, it may be resolved into two components, $\mathbf{E}_a$ and $\mathbf{E}_b$, which results in two reflected waves $\mathbf{R}_a$ and $\mathbf{R}_b$ (along **a** and **b** directions) with amplitudes determined by r_a and r_b, respectively. In the general case, the resultant electric field vector **R** for the reflected wave is elliptical. In the present case it was observed that the relative phase difference between $\mathbf{R}_a$ and $\mathbf{R}_b$ was near zero. Under this simplifying assumption (that the two

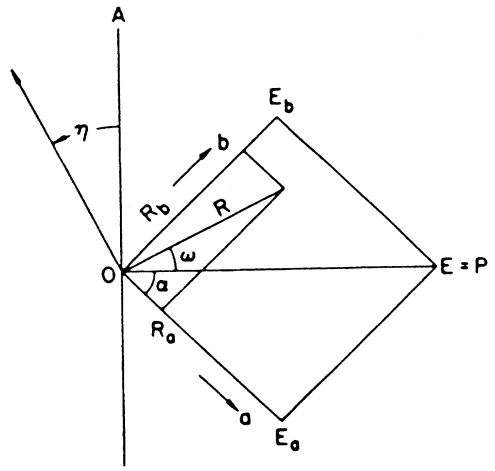

FIG. 7. Schematic diagram illustrating reflection of polarized light from a bireflecting surface, with reflectances r_a and r_b along the **a** and **b** directions. **A** and **P** denote the analyzer and polarizer, respectively. The **E** vector of the resultant reflected wave **R** is the vector sum of the two reflected waves, and is rotated an angle ω with respect to the incident wave. Hence, rotation of the analyzer through an angle η ($=\omega$) leads to complete extinction.

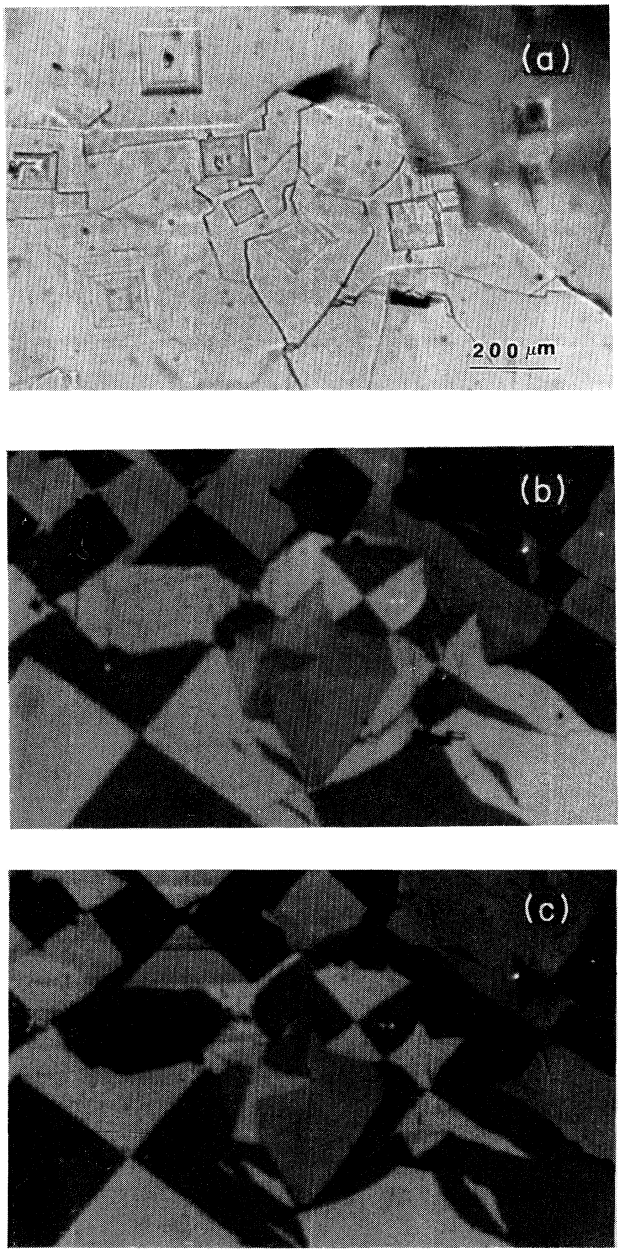

FIG. 8. Optical photomicrographs showing several twins of 2:1:2:2 on the surface of solidified flux in normal reflected light (a) and cross-polarized light (b) and (c). All of the small "crystals" had a near-square shape with growth steps similar to Fig. 1. Note that each square form had a symmetrical cruciform shape with [110] twin boundaries which nucleated from the center of the squares.

components are in phase), and using a diagonal orientation ($\alpha=45°$) such that the **E** vector of the incident polarized light is parallel to [110], complete extinction occurs on rotation of the analyzer through an angle

$$\eta=\omega=\arctan(r_b/r_a)^{1/2}-45° .$$

where

$$r_a=|\mathbf{R}_a|^2/|E_a|^2, \quad r_b=|\mathbf{R}_b|^2/|\mathbf{E}_b|^2 .$$

From the value for (r_b/r_a) determined earlier, the calculated value of $\eta=2.6°$ was in good agreement with the experimentally determined value of $\eta\approx 2.5-3°$.

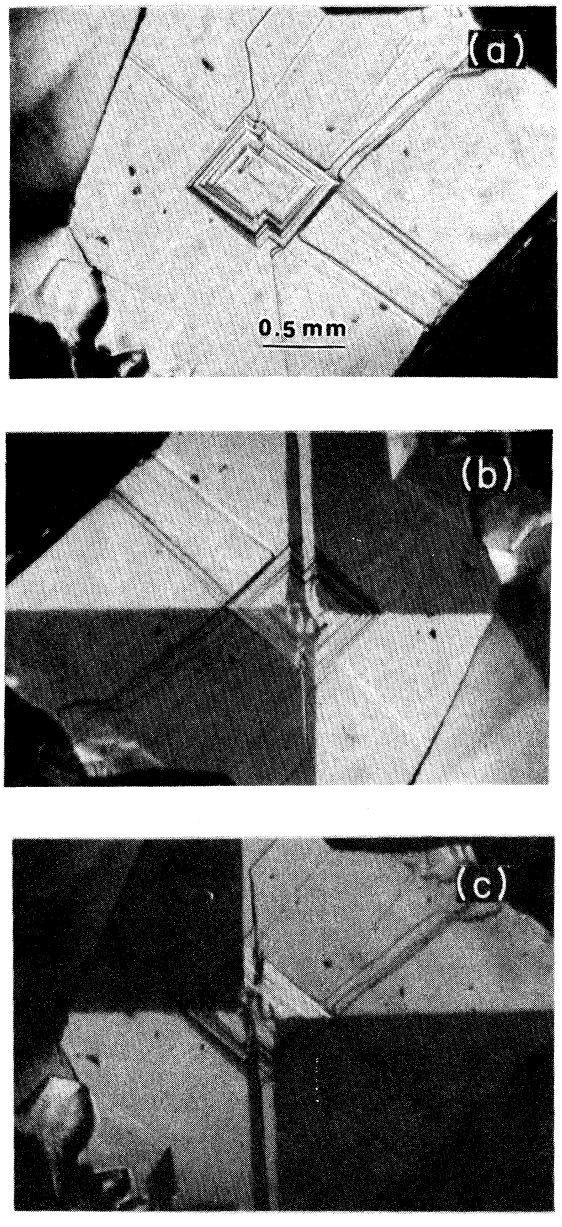

FIG. 9. Optical photomicrographs of twins originating from binuclei in normal reflected light (a) and cross-polarized light (b) and (c). The coalescence of twins during growth gave rise to an interesting extinction pattern.

Growth twinning usually occurs during the nucleation process, because the formation energy for critical nucleation is higher than the normal growth driving force, and there are more possibilities for the "accidental" emplacement of atoms or growth units into incorrect sites. In the present study, most of the twinned specimens with a cruciform shape appeared to originate from a single twinned nucleus, and in some rare cases, from twinned binuclei.

Figures 8(a)–8(c) are photomicrographs showing several twinned specimens of 2:1:2:2 on the surface of a solidified flux in normal and polarized light. The pictures were taken by the same method as for Fig. 1. Figure 8(a) is under normal reflected light, whereas, Figs. 8(b) and 8(c) are for polarized light. By comparison with Fig. 1, a careful examination reveals that all the 2:1:2:2 "crystals" with a square shape on the (001) basal plane had the following interesting features: (i) twins with symmetric cruciform shape and (110) twin boundaries, (ii) **a** axes parallel to the edges with **b** axes normal to the edges, and (iii) nucleation of each twin from the center where the {110} twin boundaries crossed.

Binuclei twins were observed on rare occasions. Figure 9 shows photomicrographs of twins originating from twinned binuclei, taken by the same procedure as in Fig. 1.

CONCLUSIONS

We have grown large-area twins of 2:1:2:2 in the Bi-Ca-Sr-Cu-O system. By means of OM, SEM and TEM, the twins were determined to be growth twins with a (110) twin boundary. The growth mechanism was by two-dimensional nucleation and layer growth on the (001) plane, after nucleation associated with {110} type twinning. Optical microscopy was used in cross-polarized light for the observation of the twins, and the determination of a bireflective optical-anisotropy ratio of ≈ 1.1. Preliminary examination of electrical resistance measurement for the twins indicates that a single (110) twin boundary did not significantly affect the resistance-temperature characteristics. On the other hand, growth steps on the (001) face had a significant effect in determining the shape and curvature of the resistance-versus-temperature characteristics. The exact nature of the twin boundary and the role of twins in flux pinning, and hence on the critical current density J_c, are perhaps more important questions in the context of structure-property relations, and future research is directed toward these issues.

ACKNOWLEDGMENTS

The authors gratefully acknowledge the support of the National Science Foundation (DMR 88-09854) through the Science and Technology Center for Superconductivity for crystal growth and electrical measurements, and to U.S. DOE DMR DE-AC02-76ER01198 for optical- and electron-microscopy studies.

[1]M. K. Wu, J. R. Ashburn, C. J. Torng, P. H. Hor, R. L. Meng, L. Gao, Z. J. Huang, Y. Q. Wang, and C. W. Chu, Phys. Rev. Lett. **58**, 908 (1987).

[2]H. Maeda, Y. Tanaka, M. Fukutomi, and T. Asano, Jpn. J. Appl. Phys. **27**, L209 (1988).

[3]Z. Z. Sheng and A. M. Hermann, Nature (London) **332**, 138 (1988).

[4]C. Michel, M. Hervieu, M. M. Borel, A. Grandin, F. Deslandes, J. Provost, and B. Raveau, Z. Phys. B **68**, 421 (1987).

[5]R. M. Hazen, C. T. Prewitt, R. J. Angel, N. L. Ross, L. W. Finger, C. G. Hadiadacos, D. R. Veblen, P. J. Heaney, P. H. Hor, R. L. Meng, Y. Y. Sun, Y. Q. Wang, Y. Y. Xue, Z. J. Huang, L. Gao, J. Bechtold, and C. W. Chu, Phys. Rev. Lett. **60**, 1174 (1988).

[6]M. A. Subramanian, C. C. Torardi, J. C. Calabrese, J. Gopalakrishnan, K. J. Morrissey, T. R. Askew, R. B. Flippen, U. Chowdhry, and A. W. Sleight, Science **239**, 1015 (1988).

[7]J-M. Tarascon, W. R. McKinnon, P. Barboux, D. M. Hwang, B. G. Bagley, L. H. Greene, G. W. Hull, Y. Le Page, N. Stoffel, and M. Giroud, Phys. Rev. B **38**, 8885 (1988).

[8]S. A. Sunshine, T. Siegrist, L. F. Schneemeyer, D. W. Murphy, R. J. Cava, B. Batlogg, R. B. van Dover, R. M. Fleming, S. H. Glarum, S. Nakahara, R. Farrow, J. J. Krajewski, S. M. Zahurak, J. V. Waszczak, J. H. Marshall, P. Marsh, L. W. Rupp, Jr., and W. F. Peck, Phys. Rev. B **38**, 893 (1988).

[9]Y. Matsui, H. Maeda, Y. Tanaka, E. Takayama-Muromachi, S. Takekawa, and S. Horiuchi, Jpn. J. Appl. Phys. **27**, L827 (1988).

[10]H. W. Zandbergen, W. A. Groen, F. C. Mijlhoff, G. van Tendeloo, and S. Amelinckx, Physica C **156**, 325 (1988).

[11]R. Herrera, J. Reyes-Gasga, P. Schabes-Retchkiman, A. Gomez, and M. J. Yacaman, Physica C **158**, 490 (1989).

[12]X. B. Kan, J. Kulik, P. C. Chow, S. C. Moss, Y. F. Yan, J. H. Wang, and Z. X. Zhao, J. Mater. Res. **5**, 731 (1990).

[13]A. Sequeira, H. Rajagopal, and J. V. Yakhmi, Physica C **157**, 515 (1989).

[14]Y. Gao, P. Lee, P. Coppens, M. A. Subramanian, and A. W. Sleight, Science **241**, 954 (1988).

[15]Y. Le Page, W. R. McKinnon, J-M. Tarascon, and P. Barboux, Phys. Rev. B **40**, 6810 (1989).

[16]C. J. Jou and J. Washburn, in *Studies of High Temperature Superconductors,* edited by A. Narlikar (Nova Science, New York, 1989).

[17]P. D. Han, A. Asthana, Z. Xu, L. Chang, and D. A. Payne, J. Mater. Res. **5**, 909 (1990).

[18]P. D. Han and D. A. Payne, J. Crystal Growth **104**, 201 (1990).

[19]Wang Jihong, Chen Genghua, Chu Xi, Yan Yifeng, Zheng Dongning, Mai Zhenhong, Yang Qiansheng, and Zhao Zhongxian, Supercond. Sci. Technol. **1**, 27 (1988).

[20]R. Galopin and N. F. M. Henry, *Microscopic Study of Opaque Minerals* (W. Heffer and Sons, Cambridge, 1972).

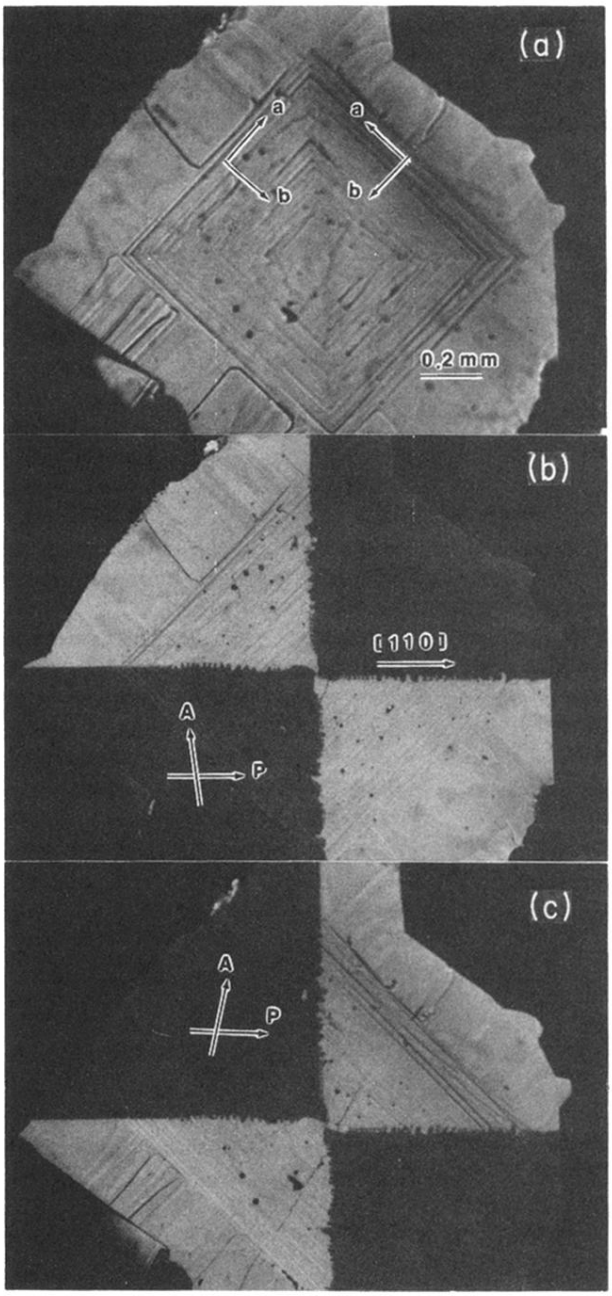

FIG. 1. Optical photomicrographs in reflected light of a cruciform twinned specimen of 2:1:2:2. (a) A characteristic near-square shape with layer growth steps parallel to [100] on the (001) face are visible in normal light. (b) Extinction of one-half (quadrants 1 and 3) was obtained between crossed polars. (Complete extinction occurred on rotation of the analyzer by 2.5–3° counterclockwise to the crossed-polars position.) (c) Extinction of the other half (quadrants 2 and 4) was obtained on rotation of the analyzer by 2.5–3° clockwise from the crossed-polars position (polarizer parallel to the [110] direction).

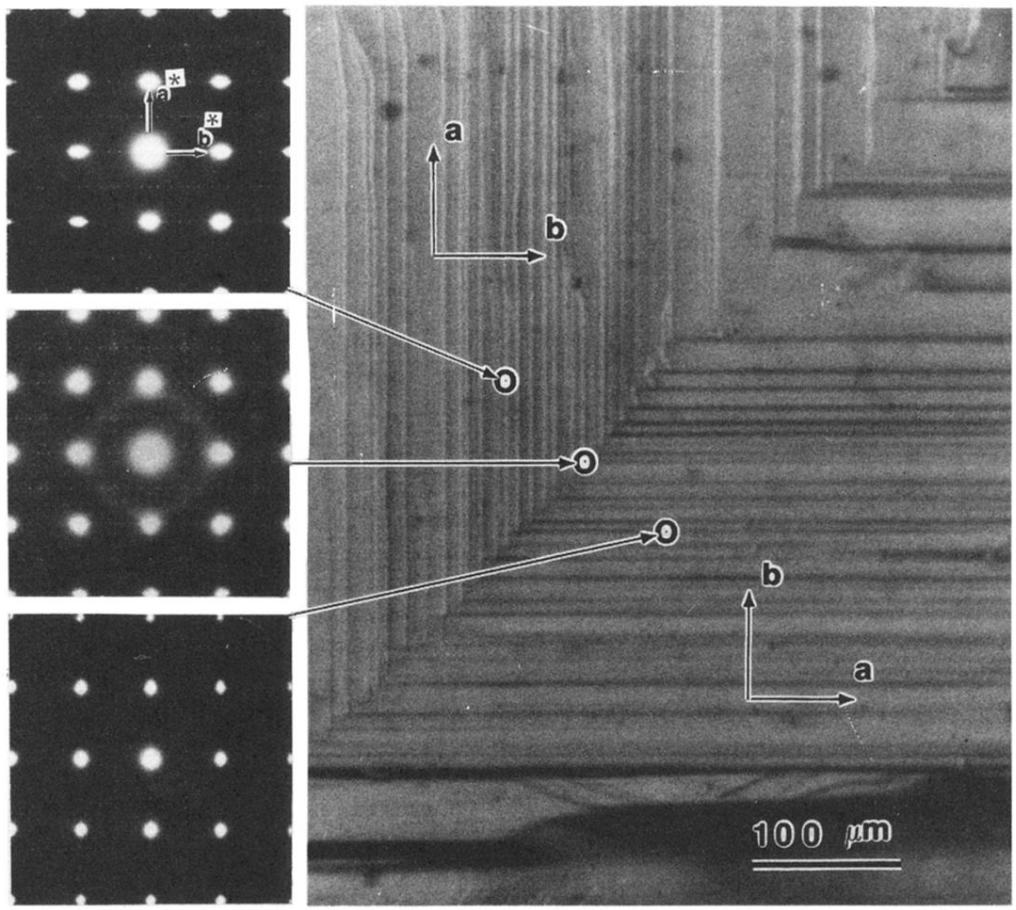

FIG. 2. (001) SAD patterns obtained from different positions in a twinned specimen. The **a** and **b** axes may easily be distinguished by the satellite spots arising from an about fivefold modulation along the [010] direction. Note that the patterns on either side of the twin boundary are similar but rotated 90° with respect to one another. The SAD pattern for the twin boundary is an overlap of the previous two patterns, as expected.

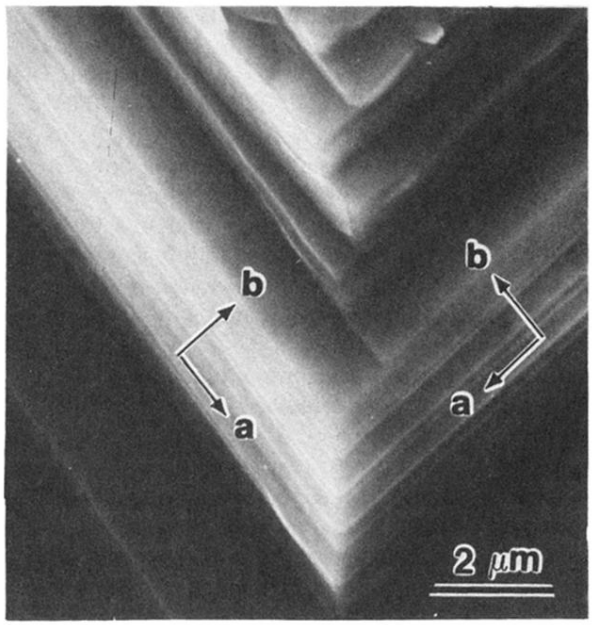

FIG. 3. SEM photomicrograph showing growth morphology of a twinned specimen. A characteristic layered structure, indicative of two-dimensional growth, is apparent. Note the disregistry between the individual growth steps, and consequent shift in the [110] boundaries, between the layers. The [110] twin boundary follows a zigzag path, as previously observed in Fig. 1.

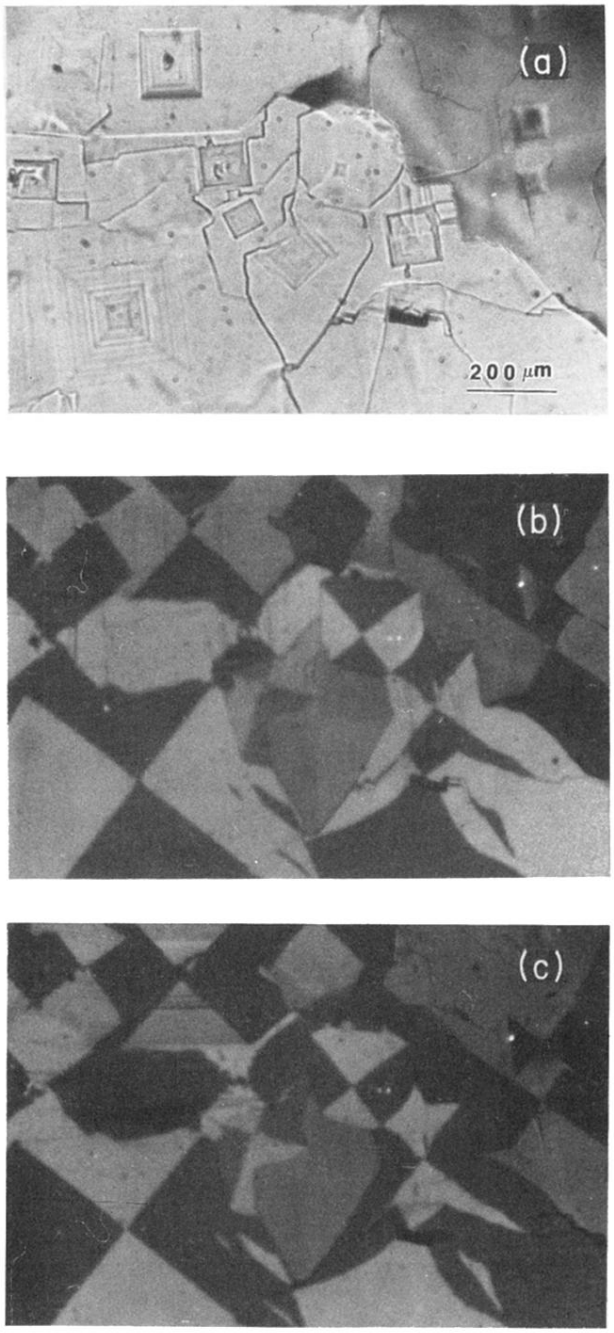

FIG. 8. Optical photomicrographs showing several twins of 2:1:2:2 on the surface of solidified flux in normal reflected light (a) and cross-polarized light (b) and (c). All of the small "crystals" had a near-square shape with growth steps similar to Fig. 1. Note that each square form had a symmetrical cruciform shape with [110] twin boundaries which nucleated from the center of the squares.

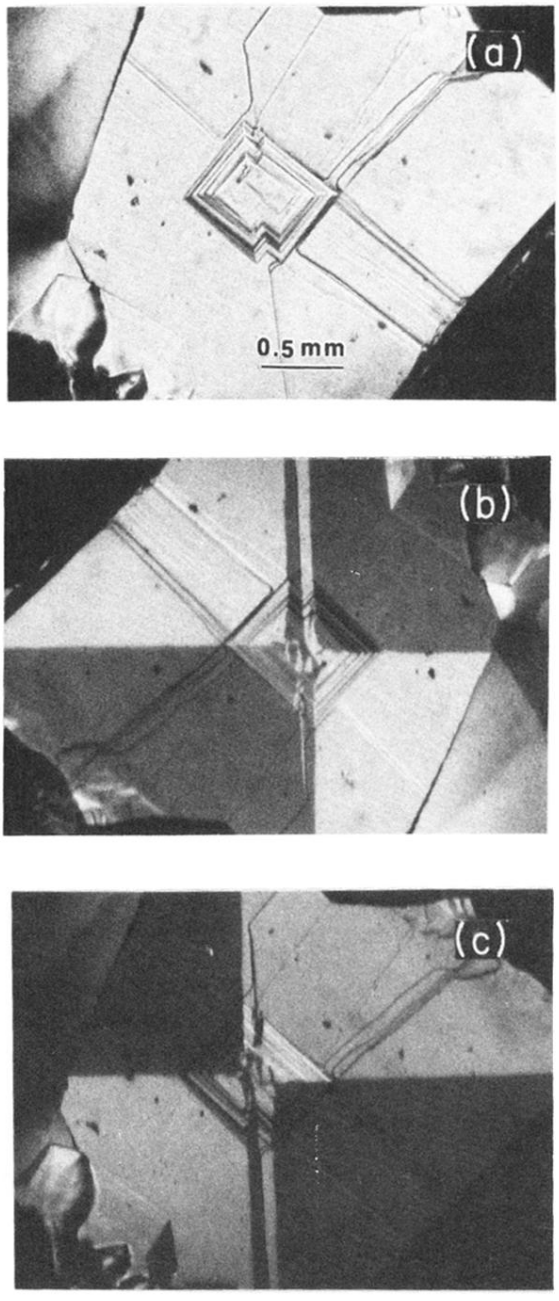

FIG. 9. Optical photomicrographs of twins originating from binuclei in normal reflected light (a) and cross-polarized light (b) and (c). The coalescence of twins during growth gave rise to an interesting extinction pattern.